

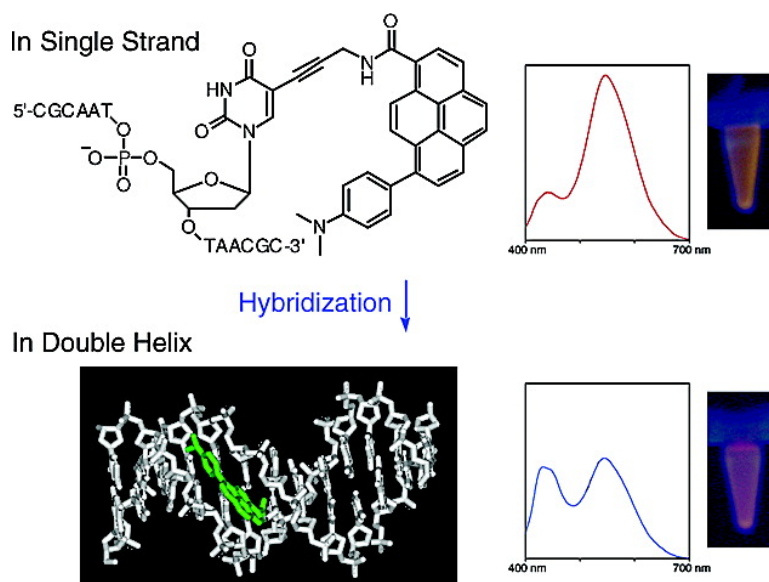
Communication

Monitoring DNA Structures by Dual Fluorescence of Pyrene Derivatives

Akimitsu Okamoto, Kazuki Tainaka, Ken-ichiro Nishiza, and Isao Saito

J. Am. Chem. Soc., **2005**, 127 (38), 13128-13129 • DOI: 10.1021/ja053609e • Publication Date (Web): 02 September 2005

Downloaded from <http://pubs.acs.org> on March 25, 2009



More About This Article

Additional resources and features associated with this article are available within the HTML version:

- Supporting Information
- Links to the 9 articles that cite this article, as of the time of this article download
- Access to high resolution figures
- Links to articles and content related to this article
- Copyright permission to reproduce figures and/or text from this article

[View the Full Text HTML](#)

Monitoring DNA Structures by Dual Fluorescence of Pyrene Derivatives

Akimitsu Okamoto,^{*,†} Kazuki Tainaka,[†] Ken-ichiro Nishiza,[†] and Isao Saito^{*,‡}

Department of Synthetic Chemistry and Biological Chemistry, Faculty of Engineering, Kyoto University, Kyoto 615-8510, and NEWCAT Institute, School of Engineering, Nihon University, and SORST, Japan Science and Technology Agency, Tamura, Koriyama 963-8642, Japan

Received June 2, 2005; E-mail: okamoto@sbchem.kyoto-u.ac.jp; saito@mech.ce.nihon-u.ac.jp

Dual fluorescence,¹ originating from two relaxed singlet excited states, a locally excited (LE) state, and an intramolecular charge transfer (ICT) state, has often been observed for electron donor/acceptor fluorophores, such as 1-arylpyrene² and 4-dialkylaminobenzonitrile derivatives.³ The equilibrium between LE and ICT states has usually been controlled by solvent temperature or viscosity depending on the height of the activation energy to the ICT state, E_a .⁴ However, a fluorophore with dual fluorescence has not been used as a fluorescent probe for biomolecules, although this unique character would be suitable for monitoring the change in the microenvironment of biomolecules by taking advantage of the color change. Designing a system that can control the equilibrium between two excited states at ambient temperature without changing the solvent properties is an unavoidable subject for developing a dual fluorescence probe.

Here, we report the detection of DNA hybridization by monitoring dual fluorescence. We tethered a pyrene derivative showing dual fluorescence to a deoxynucleoside and incorporated it into DNA. The dual fluorescence was effectively controlled by incorporation of the fluorophore into a duplex at ambient temperature. The nucleoside with dual fluorescence serves as a conceptually new fluorescent probe for monitoring hybridization of nucleic acids by a color change.

We synthesized a new pyrene derivative bearing a propargyl linker, *N*-propargyl 8-(4-(*N,N*-dimethylamino)phenyl)pyrene-1-carboxamide (**1**) (Figure 1). Subsequently, we obtained a novel fluorescent deoxyuridine **2** via Sonogashira coupling of 5-iodo-2'-deoxyuridine with **1**. Nucleoside **2** was converted to the phosphoramidite derivative, which was used for the synthesis of oligodeoxynucleotides according to a conventional DNA synthesis protocol.

The fluorescence spectra of **2**, a single-stranded oligodeoxynucleotide 5'-d(CGCAAT2TAACGC)-3' (**3**, MALDI-TOF calcd [M - H] 4304.02, found 4304.93), and **3** hybridized with the complementary DNA strand, 5'-d(GCGTTAAATTGCG)-3' (**3'**), were examined in sodium phosphate buffer (pH 7.0) on excitation at 380 nm (Figure 2a). For nucleoside **2**, a single fluorescence band was observed at 540 nm. In contrast, for the single-stranded DNA **3** and the DNA duplex **3/3'**, another fluorescence band at shorter wavelength (440 nm) was observed in addition to a band at 546 nm. In particular, for **3/3'**, the highest fluorescence intensity at 440 nm was observed. This dual fluorescence was observed not only for a hybrid with a DNA strand but also for a DNA/RNA hybrid.⁵

The two fluorescence bands at 540 and 440 nm were assigned to the ICT and LE fluorescence bands, respectively, by investigating the photophysical behavior of the pyrene fluorophore **1**. Only one broad emission band at 533 nm was observed for **1** in water on excitation at 380 nm. This emission band showed a strong solvatochromicity, which can be assigned to an ICT fluorescence, and shifted to longer wavelength in highly polar solvents (490 →

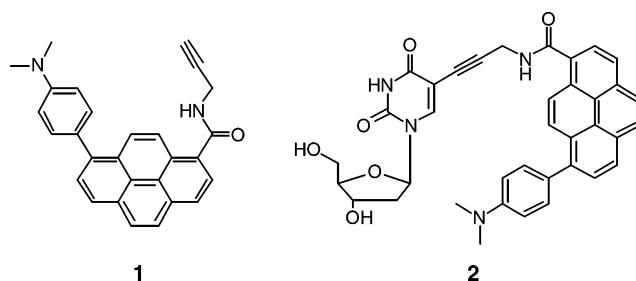


Figure 1. The structures of novel *N,N*-dimethylaminophenyl-substituted pyrene derivatives with dual fluorescence used in this study.

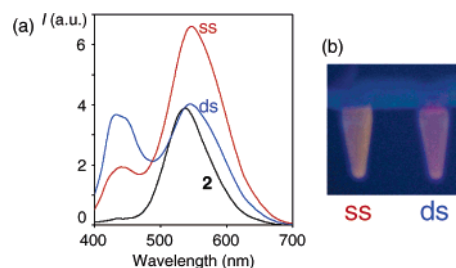


Figure 2. (a) Fluorescence spectra of 7.3 μM **2** (black line), 25 μM single strand **3** (red line), and 25 μM duplex **3/3'** (blue line) in 50 mM sodium phosphate (pH 7.0) and 0.1 M sodium chloride at 5 °C. Excitation was at 380 nm. (b) Fluorescence image of the solutions of 25 μM **3** (left) and 25 μM **3/3'** (right) illuminated with a 365 nm transilluminator.

560 nm). From a solvatochromic plot of these data for the wavenumbers of the fluorescence maxima against the solvent polarity parameter $f(\epsilon) - 1/2f(n^2)$,⁶ a dipole moment in the excited state of 18.1 D was obtained.⁵ The dipole moment greatly increased from 4.8 D in the ground state, suggesting that a large conformational change by solvent relaxation is required for transition to an ICT state.

Among three samples labeled by fluorophore **1**, the fluorophore of the duplex **3/3'** is located in a sterically restricted space. The melting temperature (T_m) of **3/3'** suggests that the fluorophore is bound to the minor groove. The duplex showed a surprisingly low T_m (41 °C), which was much lower than that of a nonmodified T/A duplex (60 °C) and close to those observed for mismatched duplexes containing 2/N base pairs (N = G, C, or T) (43–48 °C).^{5,7} It has been reported that the duplex containing a pyrene-tethered nucleotide, ^{Py}U, forms a structure in which the glycosyl bond of ^{Py}U is rotated to the *syn* conformation when ^{Py}U forms an unstable base pair.⁸ The pyrene fluorophore of ^{Py}U is located in the minor groove. If so, the degree of freedom of the fluorophore of the duplex **3/3'** would be greatly restricted. In the CD spectrum of **3/3'**, a positive CD was observed at 371 nm, suggesting that the fluorophore binds to the minor groove.⁵

Two structural states of **3** showed different visible colors. An orange-colored fluorescence was observed for the single strand state, whereas the duplex **3/3'** emitted a pink fluorescence as a mixture

[†] Kyoto University.

[‡] Nihon University.

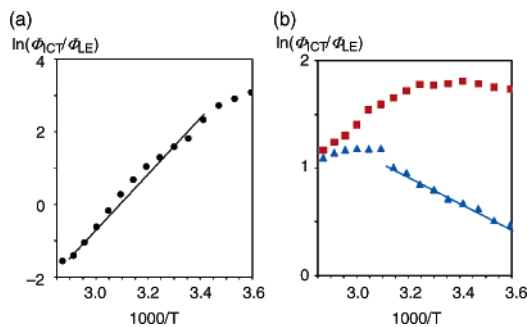


Figure 3. Stevens–Ban plot of the ICT-to-LE fluorescence intensity ratio of **2**, single strand **3**, and duplex **3/3'** in 50 mM sodium phosphate (pH 7.0) and 0.1 M sodium chloride. The temperature was changed from 5 to 75 °C; (a) 7.3 μM **2**. The line through the data points (its slope equals $-\Delta H/R$ under the high-temperature limit condition) corresponds to a stabilization enthalpy ΔH of -50.1 kJ mol $^{-1}$; (b) 25 μM **3** (red squares) and 25 μM **3/3'** (blue triangles). Because the slope of the blue straight line is $-E_a/R$ at the low-temperature limit, the activation energy, E_a , was calculated to be 9.9 kJ mol $^{-1}$.

of two colors of orange ICT and blue LE fluorescence (Figure 2b). The change in the fluorescence color vividly expresses the structural change in the microenvironment around the fluorophore by hybridization with the complementary strand. It has previously been reported that the increase in the LE versus the ICT states is connected with a conformational relaxation that can be frozen out by lowering the temperature. Our observation is very similar to this phenomenon. In our case, it is likely that the dual fluorescence of the fluorophore was strongly controlled by the duplex formation. The conformational restriction of the fluorophore in DNA induces the LE fluorescence band.

To obtain information on an excited-state equilibrium between LE and ICT states, we examined the temperature dependence of the fluorescence intensities of **2** and **3** from 5 to 75 °C. The intensity of the LE fluorescence of **2** increased with increasing temperature, whereas the ICT fluorescence intensity gradually decreased. The relation between reaction rate constants and fluorescence quantum yields is as follows:⁹

$$\Phi'(\text{ICT})/\Phi(\text{LE}) = (k'_f/k_f) \times \{k_a/(k_d + 1/\tau'_0)\} \quad (1)$$

The Stevens–Ban plot, the plots of the natural logarithm of the ICT/LE fluorescence quantum yield ratio versus the reciprocal absolute temperature,¹⁰ for **2** is shown in Figure 3a. $\Phi'(\text{ICT})/\Phi(\text{LE})$ increased upon lowering the temperature and did not deviate from linear dependence above 20 °C. This means that the high-temperature limit holds for **2**, suggesting that $1/\tau'_0$ is negligible compared with k_d , and a fast equilibrium exists between LE and ICT states after the excitation of **2**.¹¹ A value for the stabilization enthalpy, ΔH , which was obtained from the slope of this plot, was calculated as -50.1 kJ mol $^{-1}$.

The Stevens–Ban plots for the single-stranded DNA **3** and the duplex **3/3'** are shown in Figure 3b. The fluorescence behavior of **3** in the range of higher temperature (>40 °C) was similar to that of the nucleoside **2**. On the other hand, at lower temperatures, the data points tended to deviate from linearity. This indicates that the reciprocal ICT state lifetime $1/\tau'_0$ of **3** is no longer negligible with respect to k_d . It is likely that **3** partially forms a random-coiled structure, where the ICT formation is unfavorable at low temperature.

The fluorescence change for the duplex **3/3'** was quite different. The change in $\ln(\Phi'(\text{ICT})/\Phi(\text{LE}))$ behaved like that of the single strand state at temperatures higher than the duplex T_m (41 °C). The $\ln(\Phi'(\text{ICT})/\Phi(\text{LE}))$ value dropped steeply at approximately 45 °C, and then, interestingly, linearly decreased with decreasing temperature. These behaviors occurring by hybridization suggest that the fluorescence emission was under low-temperature limits, where k_d is negligibly small compared with $1/\tau'_0$.^{11a} The activation energy for the forward ICT reaction, E_a , which was calculated from the slope of the line, was estimated to be 9.9 kJ mol $^{-1}$. For phenyl-substituted pyrene derivatives, it is known that the viscosity effect of solvents strongly affects the time-determining step of twisted ICT (TICT) formation because of the irreversibility of TICT formation at low temperature.¹² In the present case, as a barrier to the internal rotation of the fluorophore, a narrow free space in the duplex structure acted instead of viscous solvents. The relaxation of the fluorophore toward TICT would be difficult in the minor groove of the duplex.

In conclusion, we have developed a conceptually new nucleoside modified by the fluorophore with dual fluorescence. The dual fluorescence was effectively controlled at ambient temperature by incorporation of the fluorophore into a duplex. The TICT formation of the fluorophore in the duplex **3/3'** was restricted by the microstructure near the fluorophore. Our nucleoside with dual fluorescence serves as a probe for monitoring hybridization with DNA or RNA by the color change without multilabeling with fluorescent dyes.

Supporting Information Available: Detailed experimental data on the synthesis and photochemical assays of the related DNA samples (in PDF format). This material is available free of charge via the Internet at <http://pubs.acs.org>.

References

- (1) Lippert, E.; Lüder, W.; Boss, H. In *Advances in Molecular Spectroscopy*; Marngini, A., Ed.; Pergamon Press: Oxford, 1962; p 443.
- (2) (a) Dobkowski, J.; Waluk, J. *Pol. J. Chem.* **1993**, *67*, 1389–1396. (b) Wiessner, A.; Hüttmann, G.; Kühnle, W.; Staeck, H. *J. Phys. Chem.* **1995**, *99*, 14923–14930. (c) Weigel, W.; Rettig, W.; Dekhtyar, M.; Modrakowski, C.; Beinhoff, M.; Schlüter, A. D. *J. Phys. Chem. A* **2003**, *107*, 5941–5947.
- (3) (a) Rettig, W. *Angew. Chem., Int. Ed. Engl.* **1986**, *25*, 971–988. (b) Grabowski, Z. R.; Rotkiewicz, K.; Rettig, W. *Chem. Rev.* **2003**, *103*, 3899–4031.
- (4) (a) Wandelt, B.; Turkewitsch, P.; Stranix, B. R.; Darling, G. D. *J. Chem. Soc., Faraday Trans.* **1995**, *91*, 4199–4205. (b) Chagnenet, P.; Plaza, P.; Martin, M. M.; Meyer, Y. H. *J. Phys. Chem. A* **1997**, *101*, 8186–8194. (c) Techert, S.; Wiessner, A.; Schmatz, S.; Staeck, H. *J. Phys. Chem. B* **2001**, *105*, 7579–7587.
- (5) See Supporting Information.
- (6) (a) Il'ichev, Y.; Kühnle, W.; Zachariasse, K. A. *Chem. Phys.* **1996**, *211*, 441–453. (b) Mothilal, K. K.; Inbaraj, J. J.; Gandhidasan, R.; Murugesan, R. *J. Photochem. Photobiol. A* **2004**, *162*, 9–16.
- (7) These mismatched duplexes also showed dual fluorescence.
- (8) (a) Okamoto, A.; Kanatani, K.; Saito, I. *J. Am. Chem. Soc.* **2004**, *126*, 4820–4827. (b) Okamoto, A.; Kanatani, K.; Saito, Y.; Saito, I. *Photomed. Photobiol.* **2004**, *26*, 77–78.
- (9) The k_a and k_d are the rate constants of the forward and reverse ICT reaction; τ'_0 is the fluorescence lifetime of ICT fluorescence, and $k_f(\text{LE})$ and $k'_f(\text{ICT})$ are radiative rate constants.
- (10) Stevens, B.; Ban, M. I. *Trans. Faraday Soc.* **1964**, *60*, 1515–1523.
- (11) (a) Leinhos, U.; Kühnle, W.; Zachariasse, K. A. *J. Phys. Chem.* **1991**, *95*, 2013–2021. (b) Druzhinin, S.; Demeter, A.; Niebauer, M.; Tauer, E.; Zachariasse, K. A. *Res. Chem. Intermed.* **1999**, *25*, 531–550.
- (12) (a) Lippert, E.; Rettig, W.; Bonacic-Koutecky, V.; Heisel, F.; Miehé, J. A. *Adv. Chem. Phys.* **1987**, *68*, 1–173. (b) Valeur, B. *Molecular Fluorescence*; Wiley-VCH: Weinheim, Germany, 2002.

JA053609E